

Description of soft diffraction in the framework of reggeon calculus. Predictions for LHC.

M.G. Poghosyan
(Torino university)

In collaboration with:

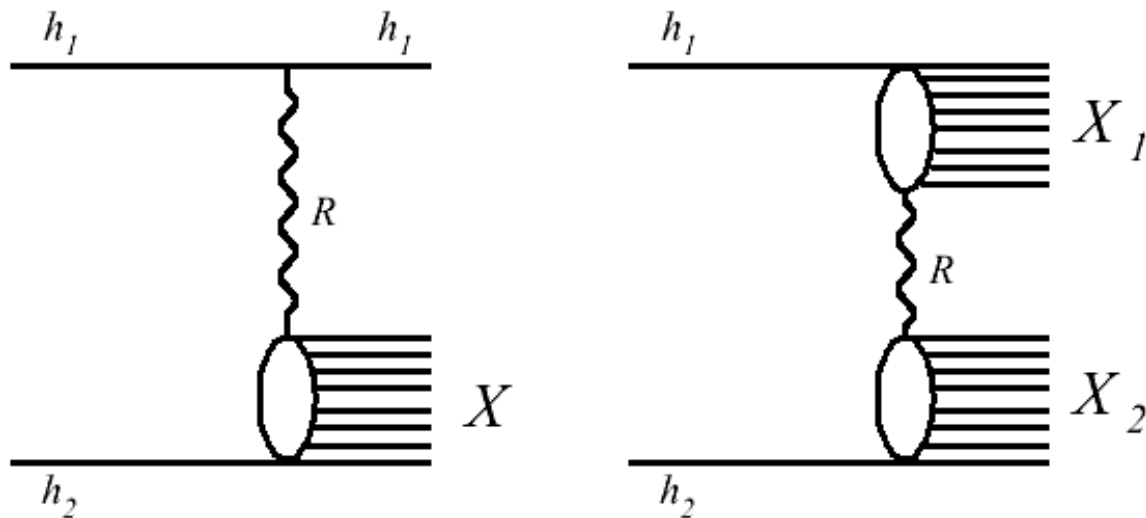
A. Kaidalov, J.-P. Revol, K. Safarik and A. Grigoryan

Regge pole exchange diagrams for SD and DD

The process of soft diffraction dissociation is closely related to small angle elastic scattering:

$$h_1 + h_2 \rightarrow h_1 + X_2, \quad h_1 + h_2 \rightarrow X_1 + h_2, \quad h_1 + h_2 \rightarrow X_1 + X_2,$$

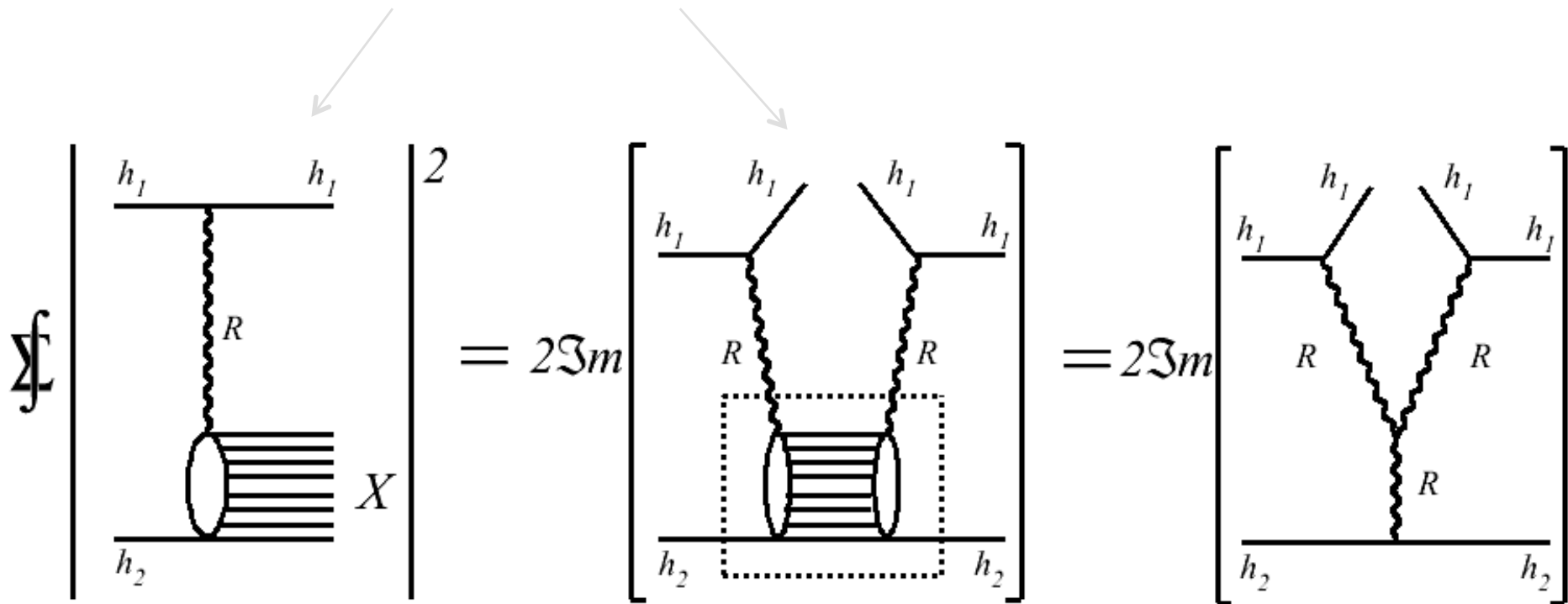
where these processes may be considered as binary reactions where each of the incoming hadrons may become a system which will then decay into a number of stable final state particles.



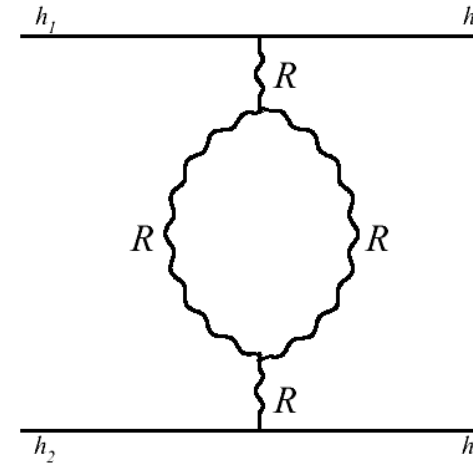
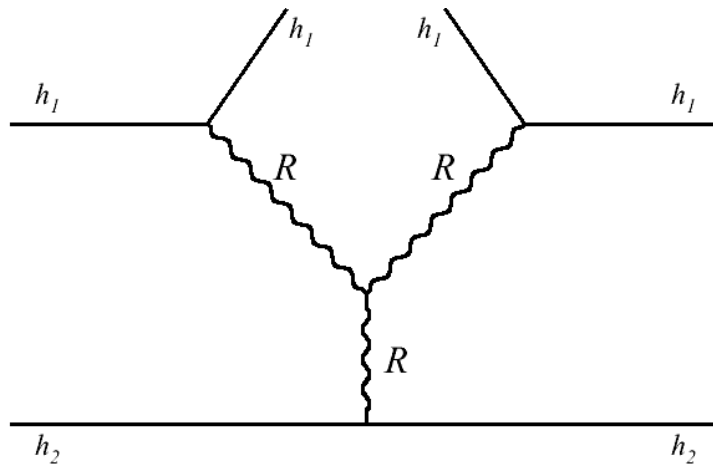
Triple-Reggeon coupling

Analogous to the optical theorem, Muller's theorem relates the inclusive cross-section for the reaction $h_1+h_2 \rightarrow h_1+X$ to the forward scattering amplitude of the three-body hadronic process $h_1+h_2+h_1 \rightarrow h_1+h_2+h_1$.

$$\sum_c T_{ac} T_{ac}^* = 2 \Im m T_{aa}$$



Triple-Reggeon and loop diagrams

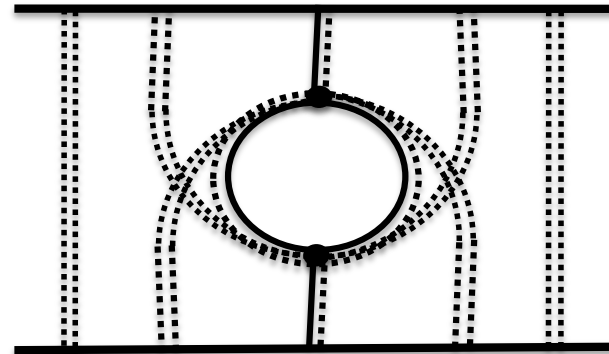
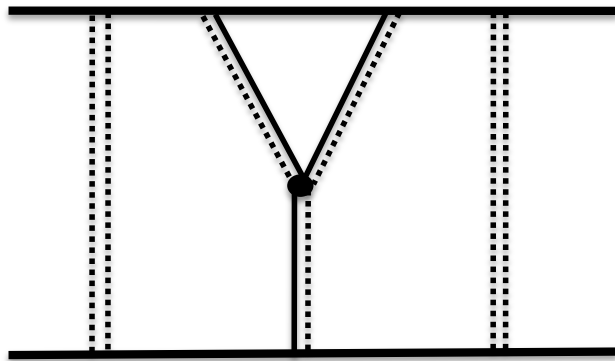


Triple-Regge description is in good agreement with the FNAL and ISR data for soft diffraction dissociation. However,

1. higher-energy data from SPS and Tevatron do not show a fast increase of the cross-section with energy as expected from the fits
2. It is not possible to have a unified description of SD and DD data.
3. The contribution of triple-Pomeron vertex leads to the violation of unitarity which requires that the total cross section at very high energies should not grow faster than $\ln^2 s$ (Froissart bound).

A model for describing high mass diffractive dissociation.

Dressed triple-Reggeon and loop diagrams



where

$$\begin{array}{c}
 \text{Diagram 1} \\
 \equiv \\
 \text{Diagram 2} + \text{Diagram 3} + \text{Diagram 4} + \dots
 \end{array}$$

The equation shows the decomposition of a dressed triple-Reggeon diagram (left) into a sum of diagrams (right). The first diagram on the right has a wavy line labeled P or R . The second has two wavy lines labeled P or R and P . The third has three wavy lines labeled P or R , P , and P . Ellipses indicate further terms in the series.

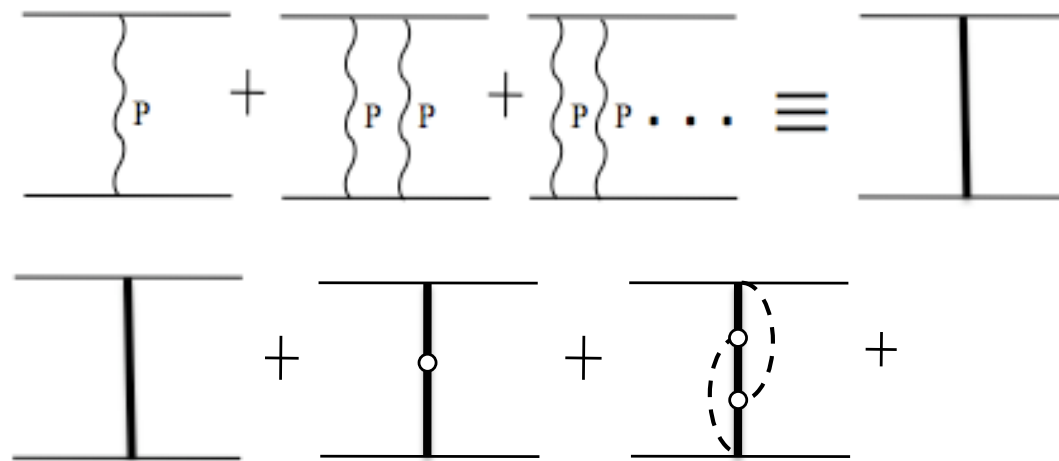
$$\begin{array}{c}
 \text{Diagram 1} \\
 \equiv \\
 \mathbf{1} + \text{Diagram 2} + \text{Diagram 3} + \text{Diagram 4} + \dots
 \end{array}$$

The equation shows the decomposition of a loop diagram (left) into a sum of diagrams (right). The first term is the identity $\mathbf{1}$. The second diagram has one wavy line labeled P . The third has two wavy lines labeled P and P . The fourth has three wavy lines labeled P , P , and P . Ellipses indicate further terms in the series.

The motivation of writing different amplitudes for SD and DD (Ren. Pomeron)

Enhanced graphs and Pomeron intercept renormalization

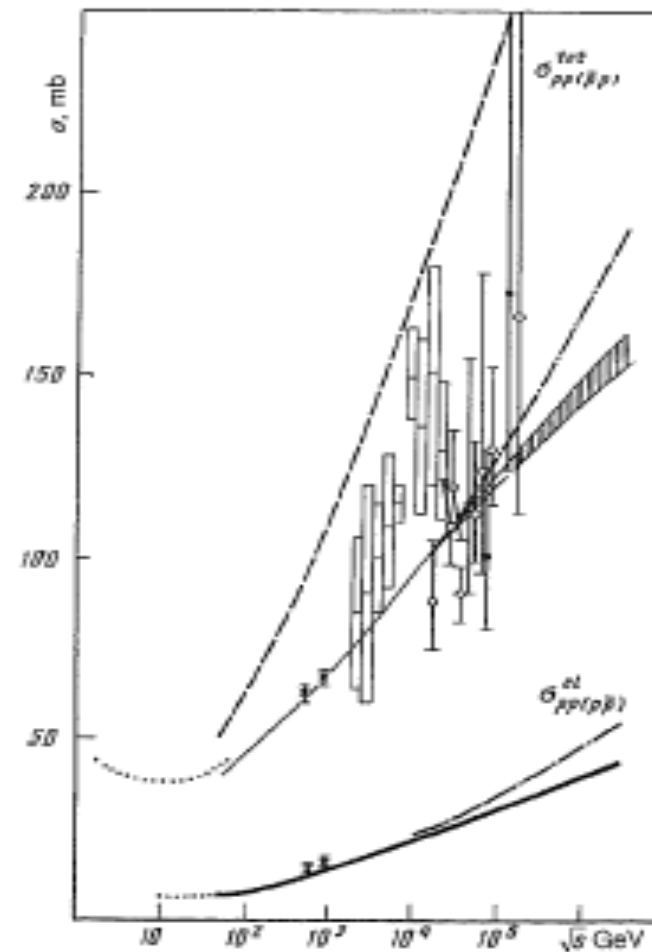
Kaidalov et al., Sov. J. N.P. 44 (KT-MP)



$$\Delta_{eff} = \Delta - 4\pi G_{PPP}$$

$$\Delta_{eff} \approx 0.12$$

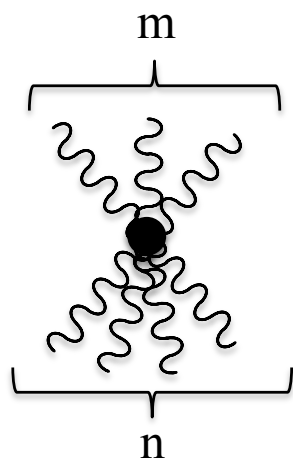
Kaidalov et al., Sov. J. N.P. 44



The assumptions used for calculating the diagrams.

1. Eikonal approximation.

2. Transition of n Pomertons into m Pomerons is dominated by pions.



$$\lambda_{n1,n2} = r_{3P} g_{\pi}^{n1+n2-3} \exp\left(-R_{\pi}^2 \sum_{i=1}^{n1+n2} k_i^2\right).$$

3. As a secondary Regge pole we consider f -trajectory. The conservation laws allow to assume the same pion dominance at transition with participation of f .

SD cross section

$$\frac{d\sigma}{d\zeta} = \sum_{i,j,k=P,R} \frac{G_{ijk}}{4\pi g_{\pi b}^i g_{\pi b}^j g_{\pi a}^k} \int d\mathbf{b} d\mathbf{b}_1 \Gamma_{b\pi}^i(\zeta_2, \mathbf{b}_2) \Gamma_{b\pi}^j(\zeta_2, \mathbf{b}_2) \Gamma_{a\pi}^k(\zeta, \mathbf{b}_1) e^{-2\Omega_{ab}(\xi, \mathbf{b})}$$

$$\xi = \ln(s/s_0), \quad \zeta = \ln(M_X^2/s_0), \quad \zeta_2 = \xi - \zeta, \quad \mathbf{b}_2 = \mathbf{b} - \mathbf{b}_1,$$

$$\Gamma_{\alpha\beta}^R(\zeta, \mathbf{b}) = \frac{g_{\alpha\beta}^R}{\lambda_{\alpha\beta}^R} \exp \left\{ (\alpha_R - 1)\zeta - \frac{\mathbf{b}^2}{4\lambda_{\alpha\beta}^R} - \Omega_{\alpha\beta}(\zeta, \mathbf{b}) \right\},$$

$$\Gamma_{\alpha\beta}^P(\zeta, \mathbf{b}) = 1 - e^{-\Omega_{\alpha\beta}(\zeta, \mathbf{b})}, \quad \Omega_{\alpha\beta}(\zeta, \mathbf{b}) = \frac{g_{\alpha\beta}}{\lambda_{\alpha\beta}} \exp \left\{ \Delta\zeta - \frac{\mathbf{b}^2}{4\lambda_{\alpha\beta}} \right\}.$$

Note our normalization of G_{ijk} is not standard.

$G_{PPP} = 2\pi g_{N\pi}^3 G$: G used in A.B. Kaidalov et al, Yad.Fiz.44

$G_{PPP} = 2g_N^3 r_{PPP}$: r_{PPP} used in A.B. Kaidalov, PRP50

Extraction of parameters from experimental data

We have 18 free parameters. In order to be close to the reality they are found as follows.

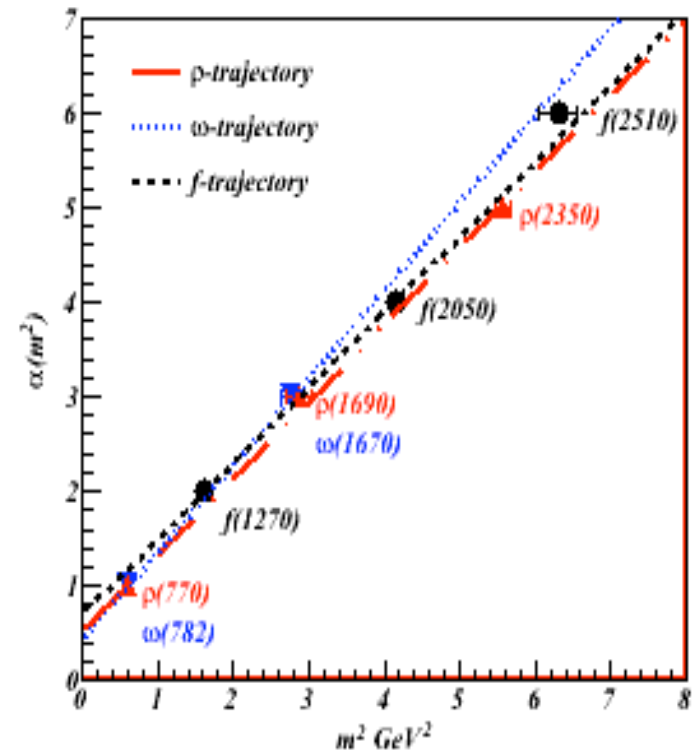
1. Regge trajectory of the f meson: $\alpha_f(t) = \alpha_f + \alpha_f' t$

The parameters are defined from data on spin vs mass.

2. The residues of f -trajectory and the residues/trajectory of the Pomeron are found from fit to data on pp, ppbar and $p\pi^\pm$ total interaction and elastic scattering cross-section.

3. Triple-reggeon constants (G_{ijk}) are found from fit to data on high mass diffraction dissociation data.

Chew-Frautschi plot



$$\alpha_i(t) = \alpha_i(0) + \alpha'_i t$$

$$\alpha_f(0) = 0.703 \pm 0.023$$

$$\alpha_\rho(0) = 0.522 \pm 0.009$$

$$\alpha_\omega(0) = 0.435 \pm 0.033$$

$$\alpha'_f = 0.797 \pm 0.014 \text{ GeV}^{-2}$$

$$\alpha'_\rho = 0.809 \pm 0.015 \text{ GeV}^{-2}$$

$$\alpha'_\omega = 0.923 \pm 0.054 \text{ GeV}^{-2}$$

pp and $p\bar{p}$ interaction parameters

$$pp = P + f - \omega$$

$$p\bar{p} = P + f + \omega$$

$$g_N = 1.366 \pm 0.004 \text{ GeV}^{-2}$$

$$R_N^2 = 1.428 \pm 0.006 \text{ GeV}^{-2}$$

$$g_N^f = 2.871 \pm 0.008 \text{ GeV}^{-2}$$

$$R_N^{f2} = 0.918 \pm 0.023 \text{ GeV}^{-2}$$

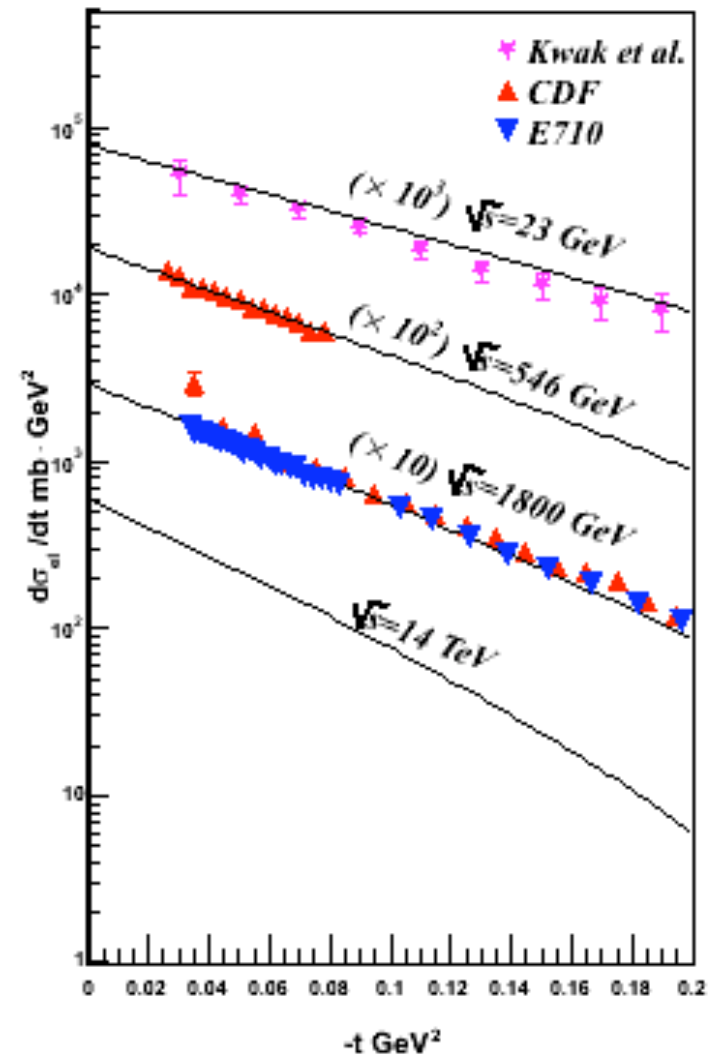
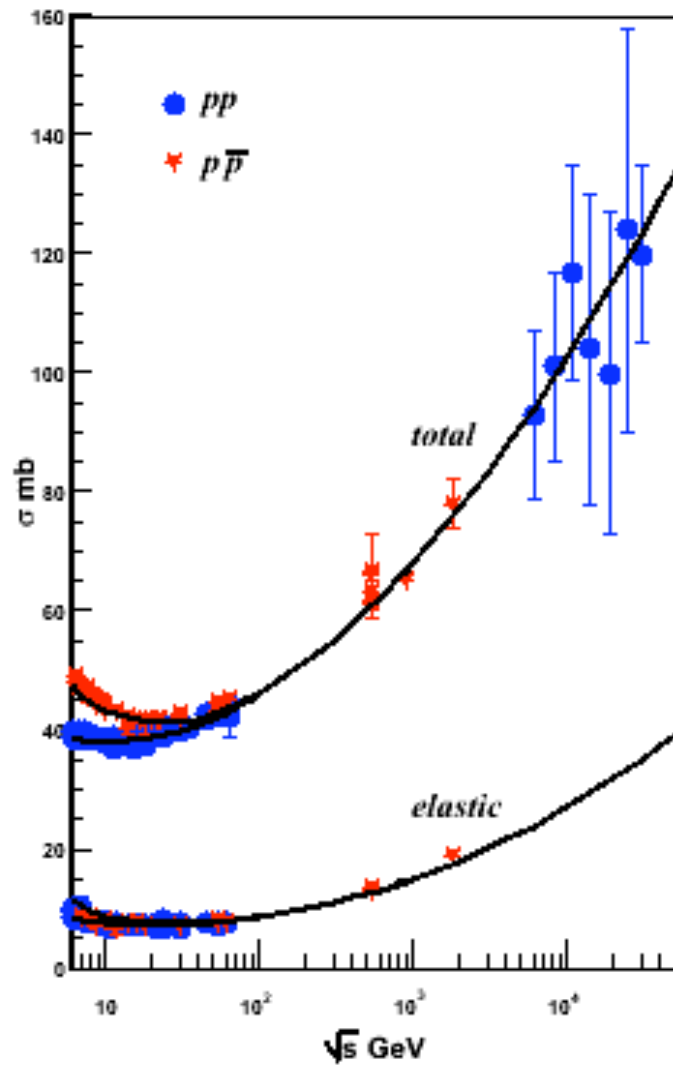
$$g_N^\omega = 2.241 \pm 0.074 \text{ GeV}^{-2}$$

$$R_N^{\omega2} = 0.945 \pm 0.026 \text{ GeV}^{-2}$$

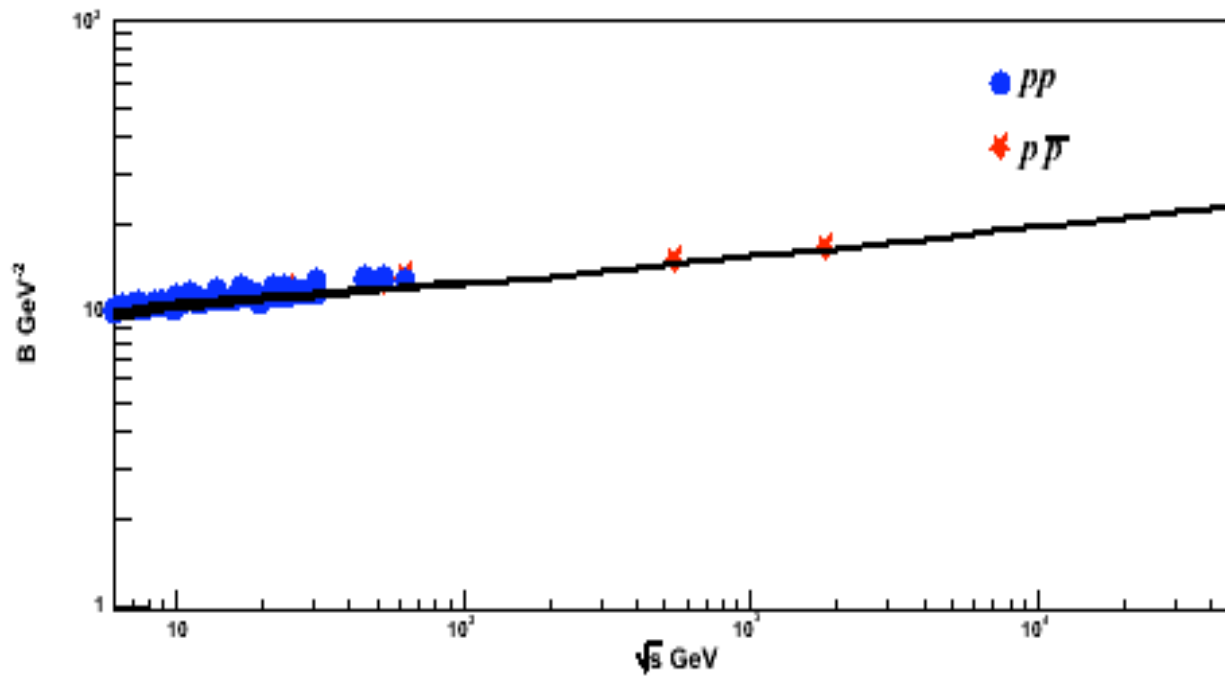
$$\Delta = 0.117 \pm 0.001$$

$$\alpha'_P = 0.252 \pm 0.003 \text{ GeV}^{-2}$$

Fit to data



Elastic scattering slope (cross-check)



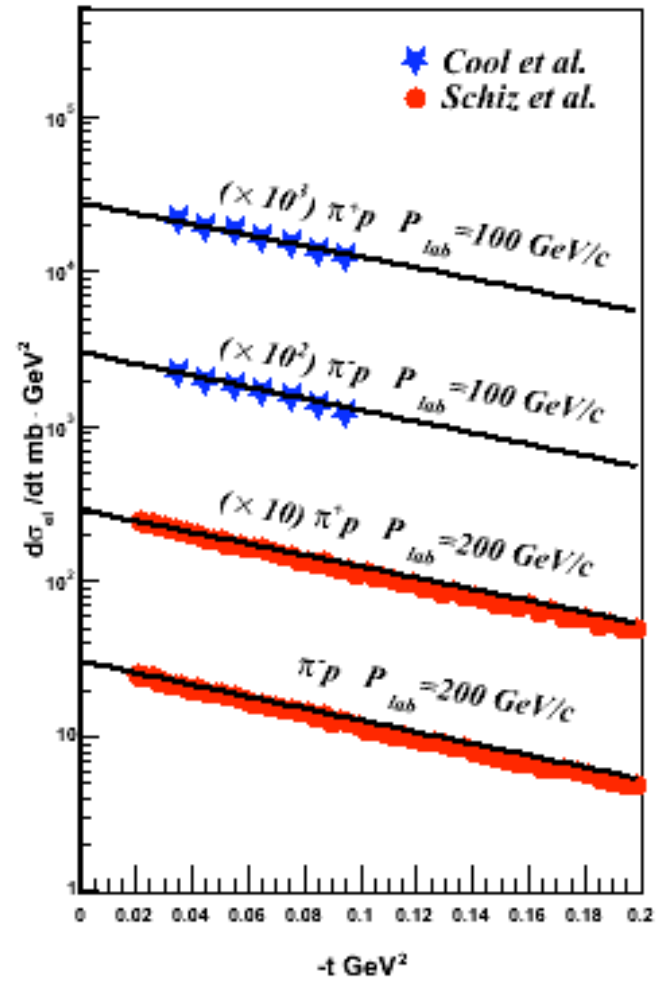
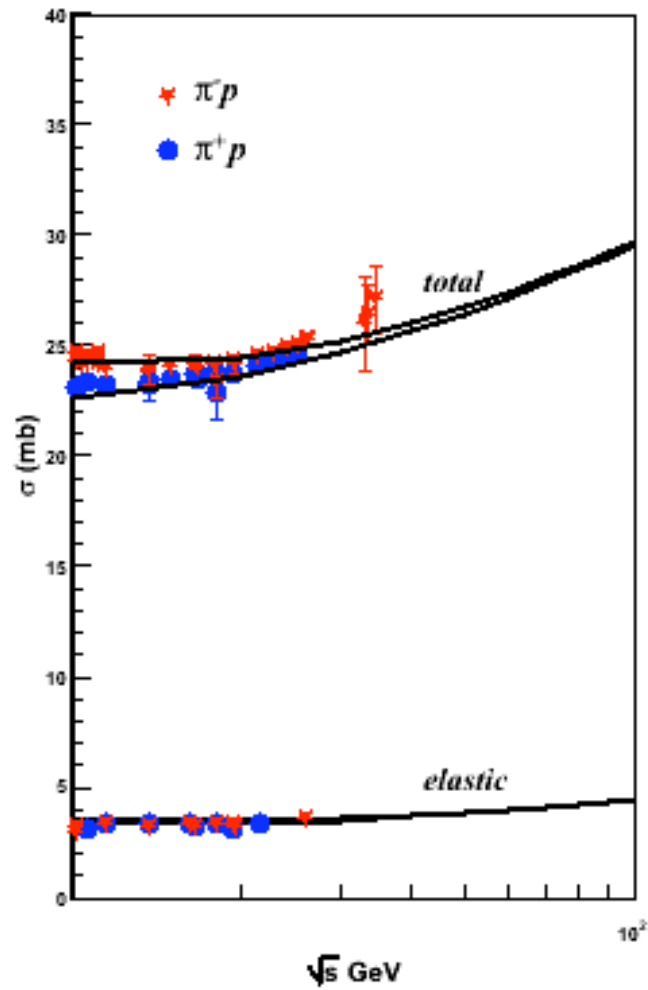
$\pi^\pm p$ interaction parameters

$$\pi^+ p = P + f - \rho$$

$$\pi^- p = P + f + \rho$$

$$\begin{aligned} g_\pi &= 0.848 \pm 0.0004 \text{ GeV}^{-2} \\ R_\pi^2 &= 0.5 \pm 0.002 \text{ GeV}^{-2} \\ g_{N\pi}^f &= 3.524 \pm 0.0009 \text{ GeV}^{-2} \\ R_{N\pi}^{f2} &= 1.0 \pm 0.0007 \text{ GeV}^{-2} \\ g_{N\pi}^\rho &= 1.118 \pm 0.0167 \text{ GeV}^{-2} \\ R_{N\pi}^{\rho2} &= 9.19 \pm 0.837 \text{ GeV}^{-2} \end{aligned}$$

Fit to data



Triple-Reggeon vertices strengths

In the next step we fix triple-Reggeon vertex strengths (G_{ijk}) from data on soft diffraction dissociation in pp and ppbar interactions. In order to do it, in addition to dressed triple-Reggeon diagrams we took into account π -meson exchange on the basis of the OPER model (the details can be found in the Appendix).

$$G_{PPP} = 0.096 \pm 0.005 \text{ GeV}^{-8}$$

$$G_{PPR} = 0.89 \pm 0.011 \text{ GeV}^{-8}$$

$$G_{RRP} = 0.49 \pm 0.078 \text{ GeV}^{-8}$$

$$G_{RRR} = 13.7 \pm 0.43 \text{ GeV}^{-8}$$

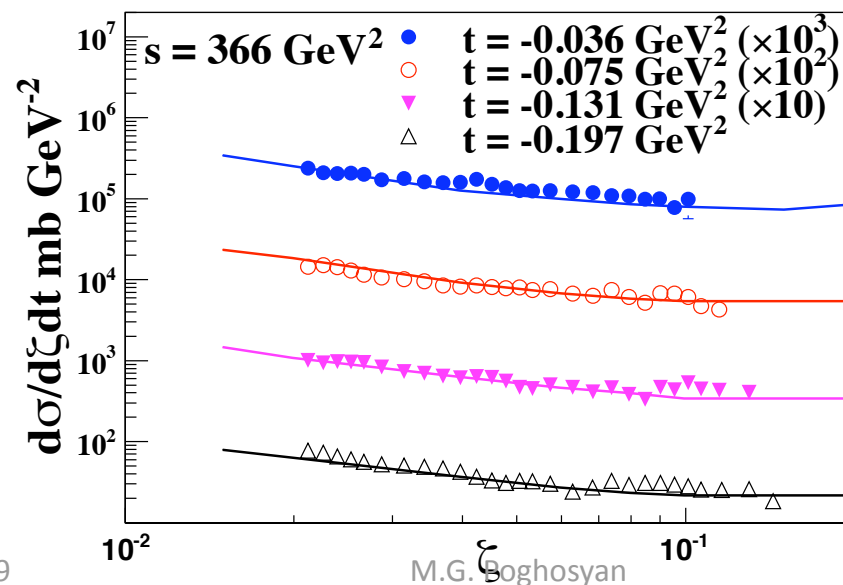
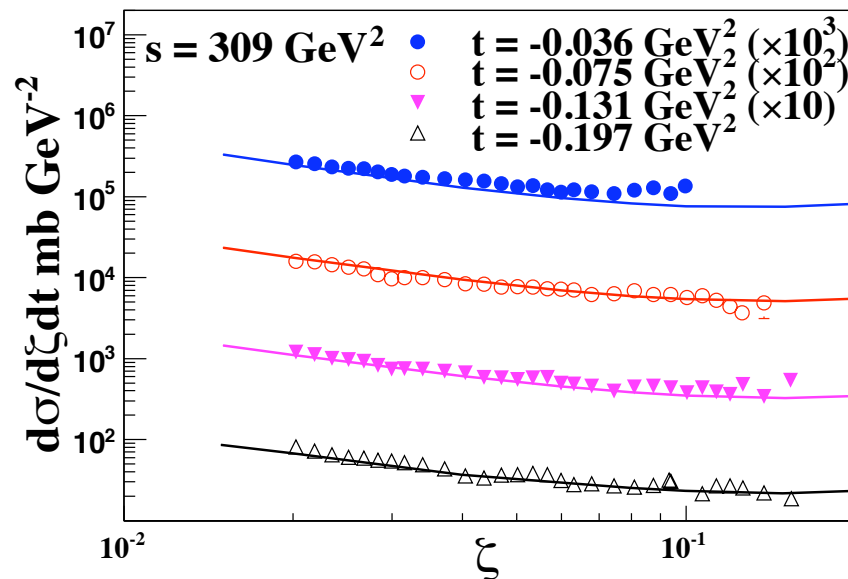
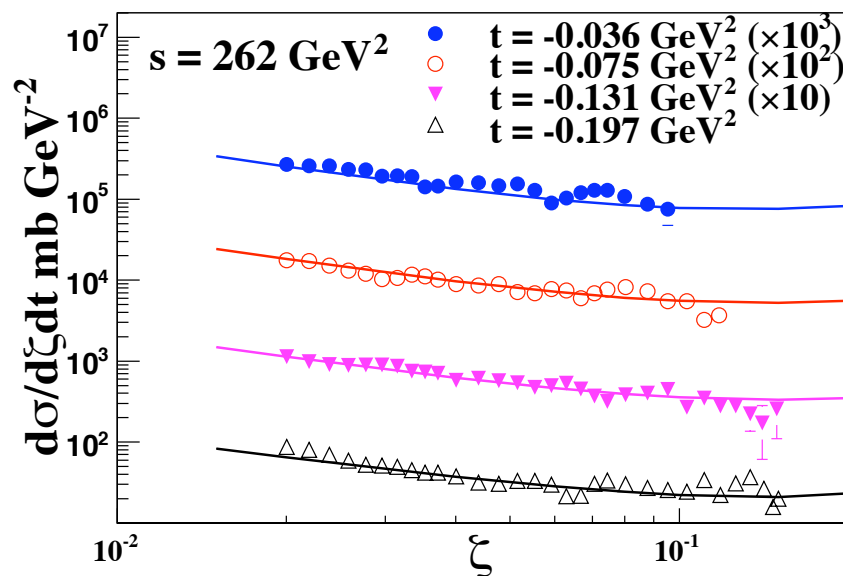
$$G_{PRP} = 0.39 \pm 0.02 \text{ GeV}^{-8}$$

$$G_{PRR} = 2.99 \pm 0.04 \text{ GeV}^{-8}$$

$$G_{PPP}/2\pi g_{N\pi}^3 = 0.0098 \text{ GeV}^{-2} \text{ (KT-MP used } 0.0135 \text{ GeV}^{-2} \text{ !)}$$

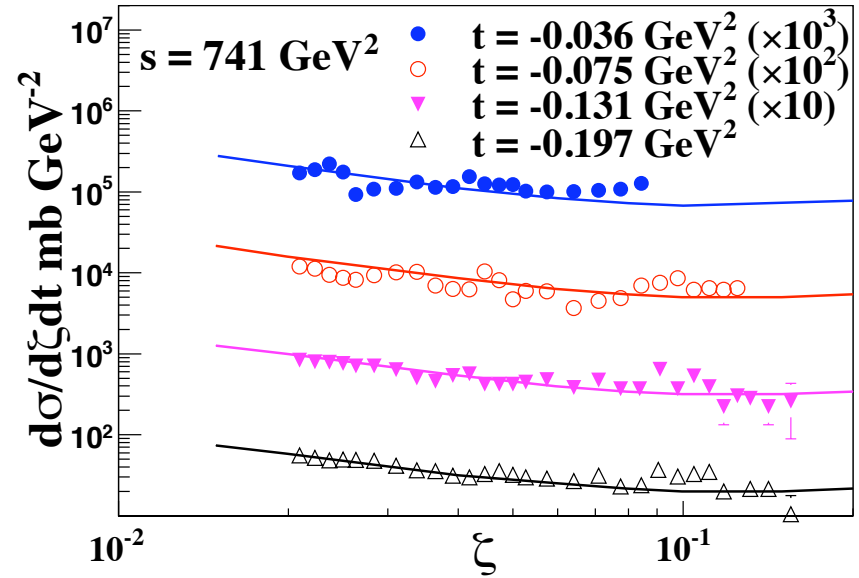
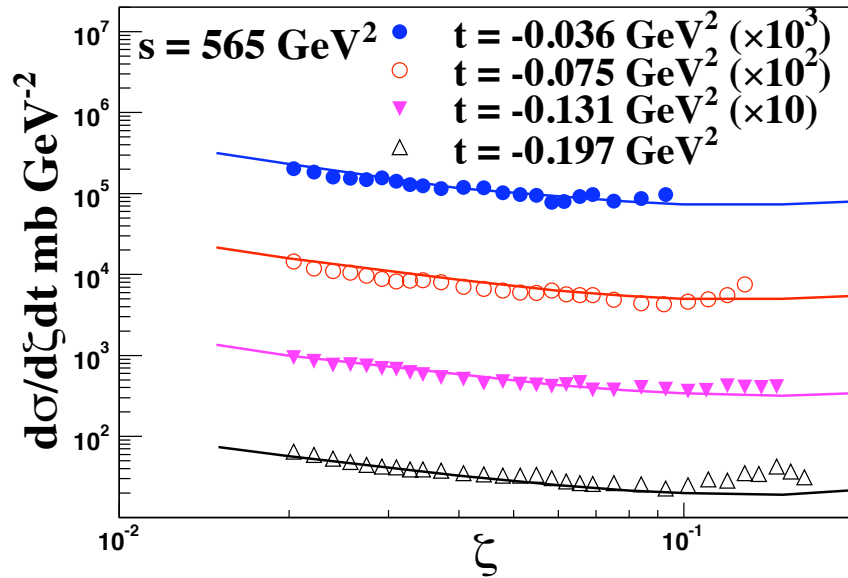
Fit to data on single diffraction dissociation

Data from Fermilab; Schamberger et al., Phys. Rev. D17



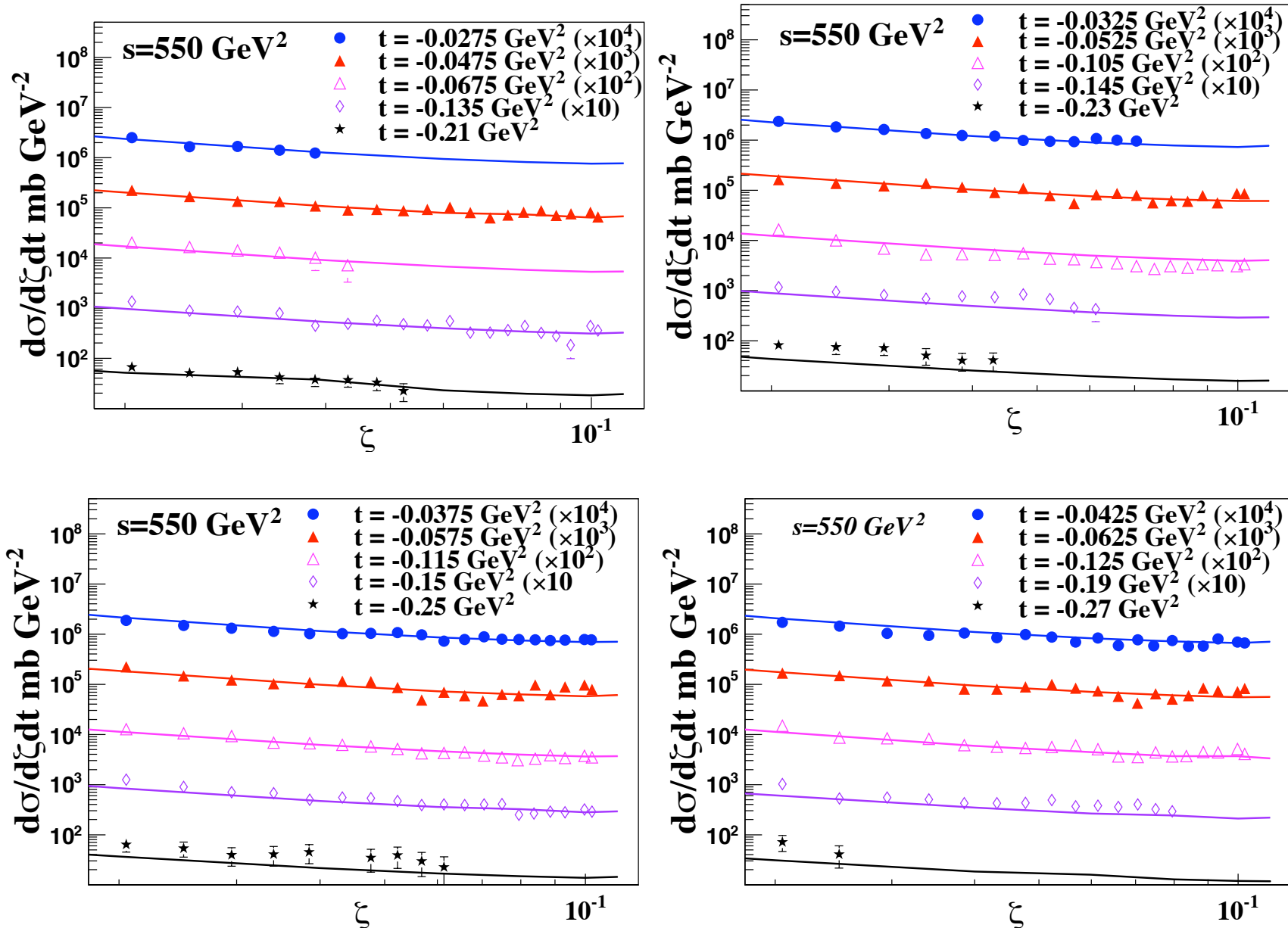
Fit to data on single diffraction dissociation

Data from Fermilab; Schamberger et al., Phys. Rev. D17

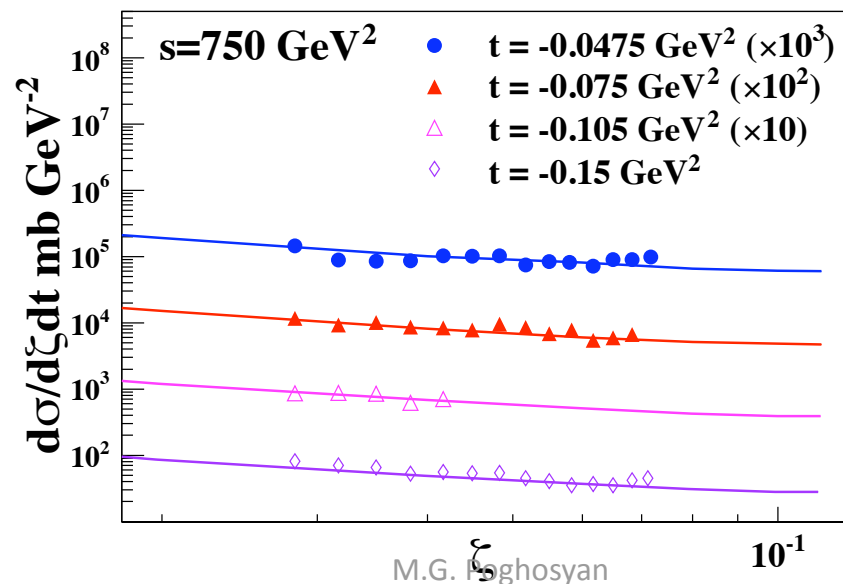
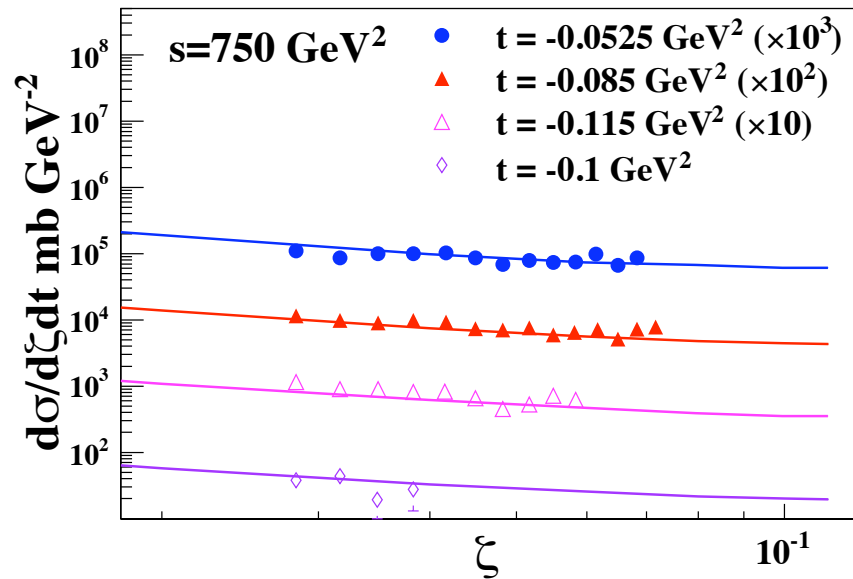
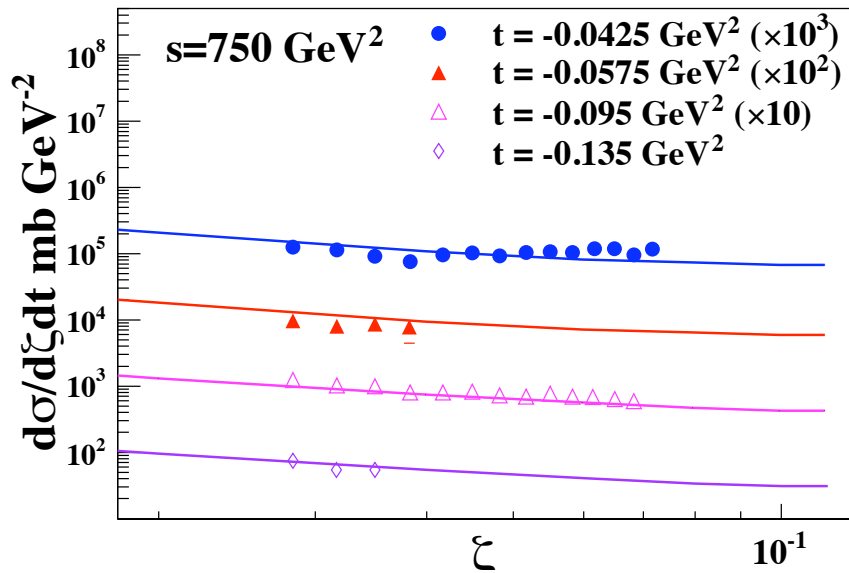


Fit to data on single diffraction dissociation

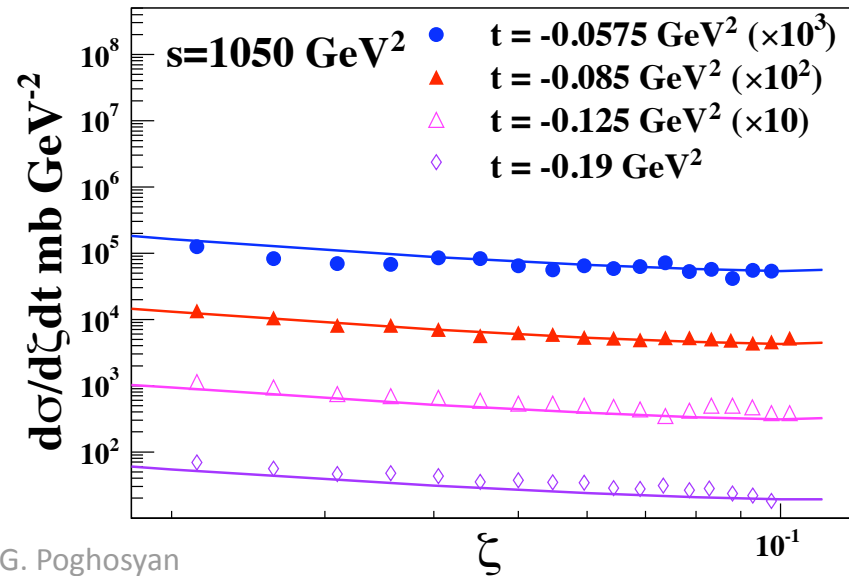
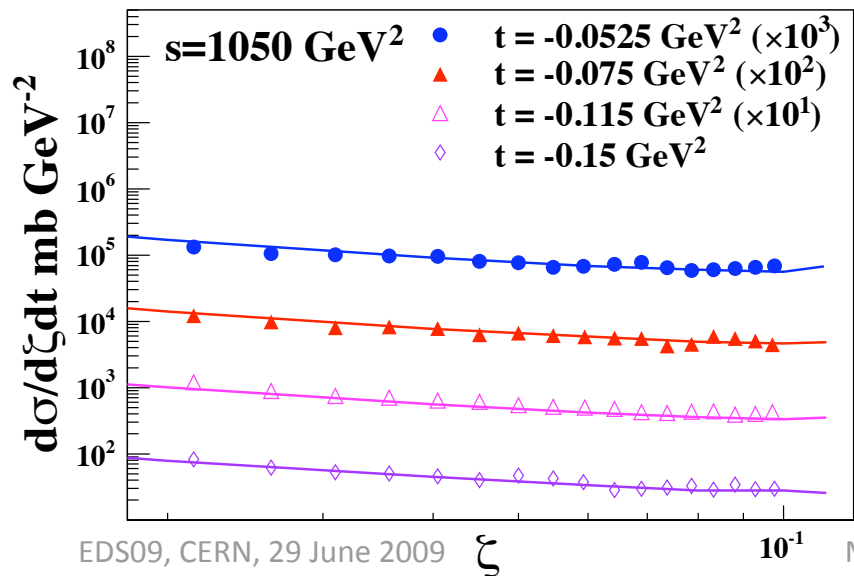
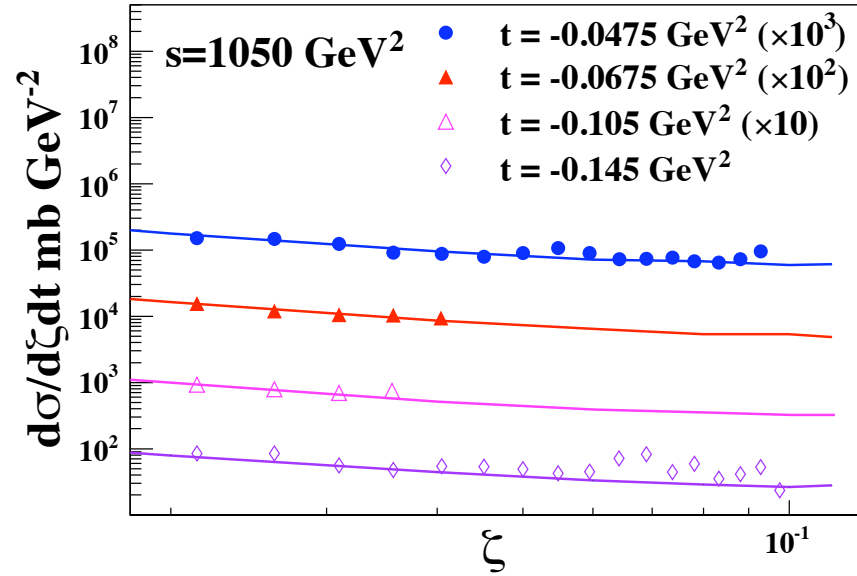
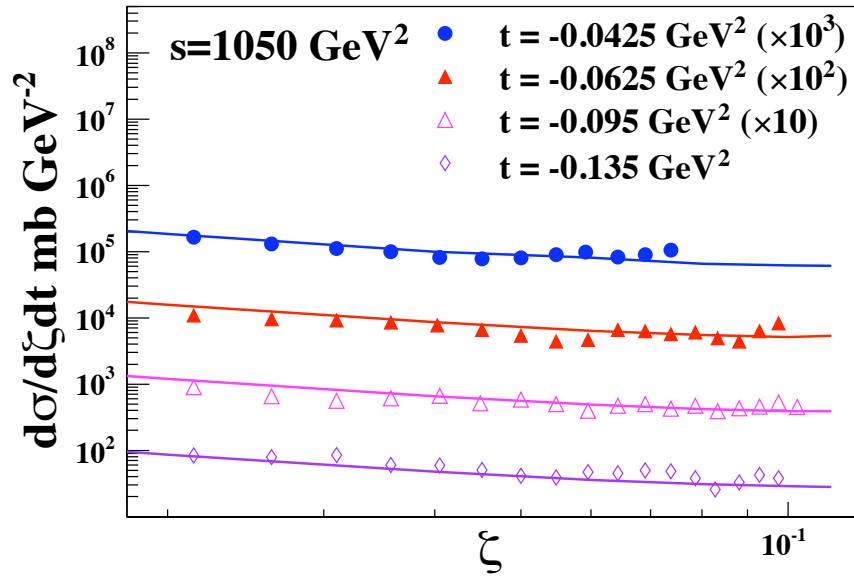
ISR data, Armitage et al. NP B194



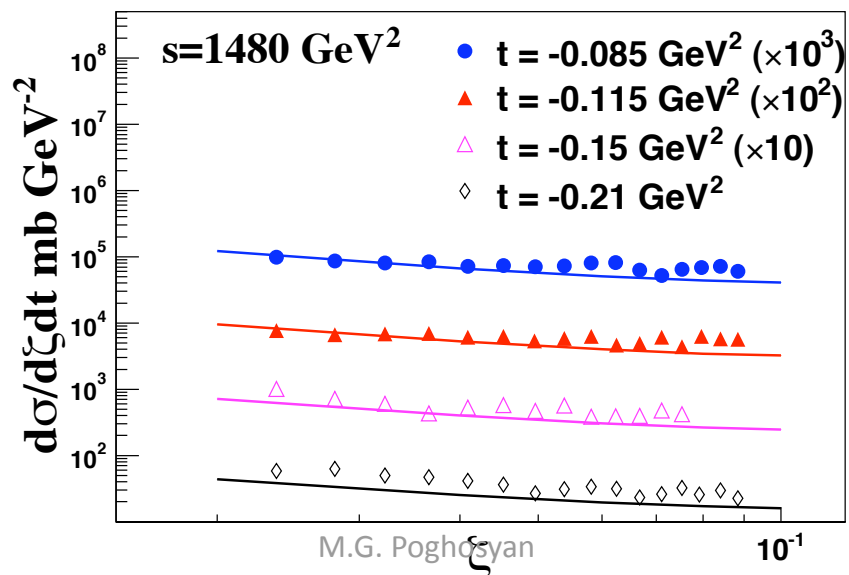
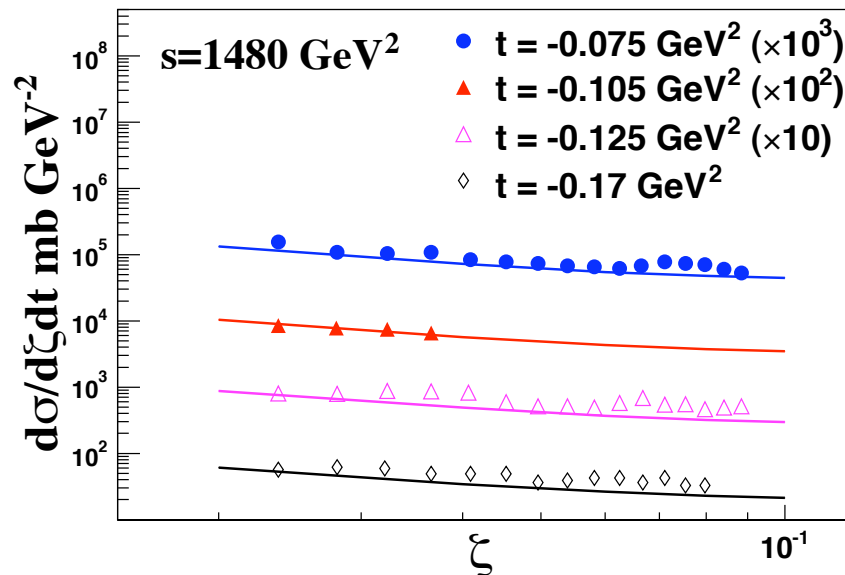
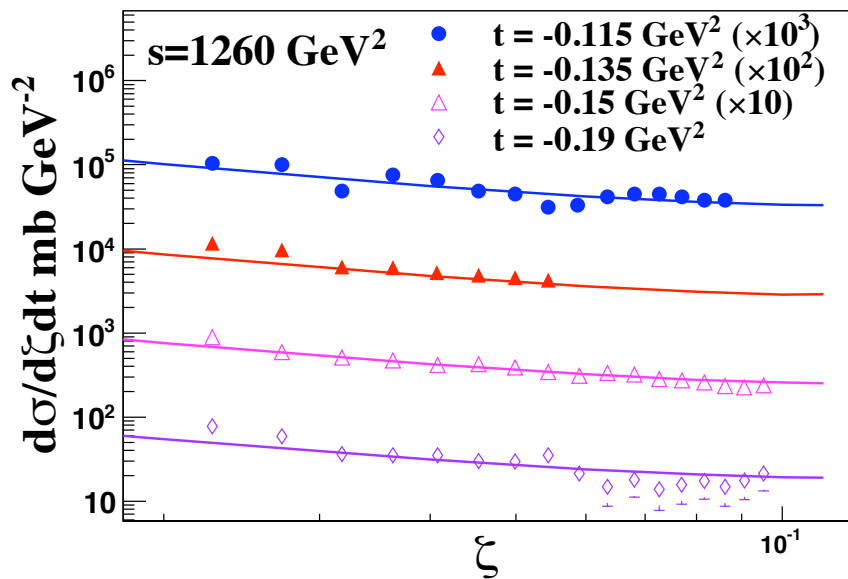
Fit to data on single diffraction dissociation



Fit to data on single diffraction dissociation



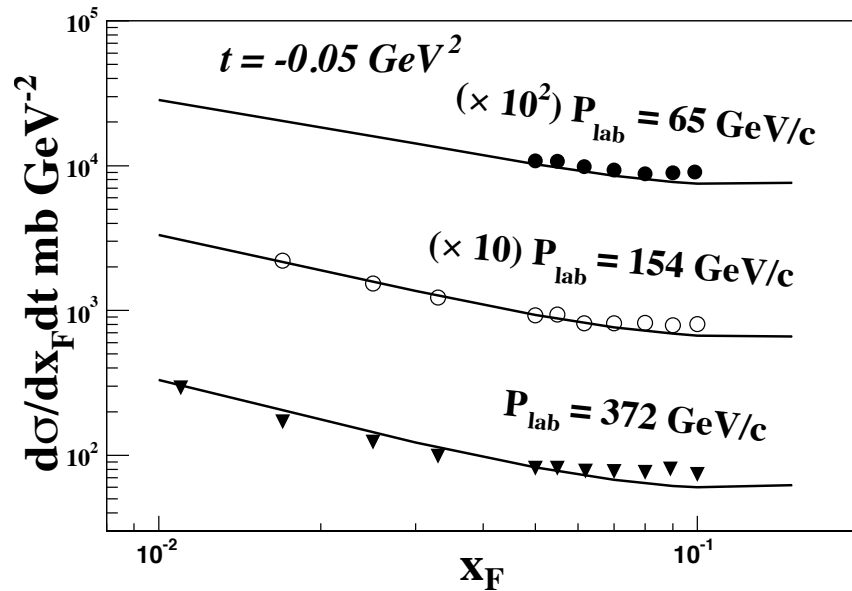
Fit to data on single diffraction dissociation



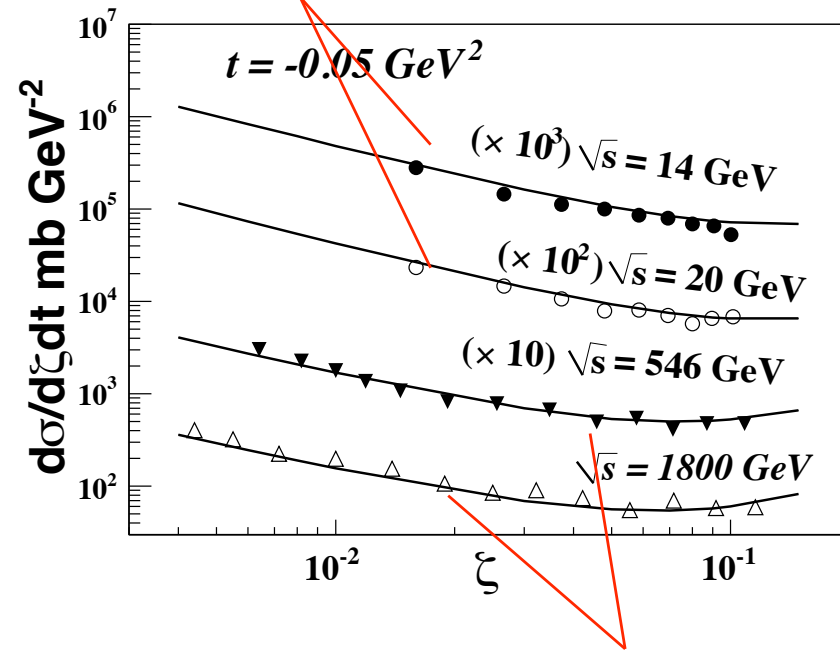
Fit to data on single diffraction dissociation

Data from Fermilab (fixed t)

Akimov et al. PRL 39

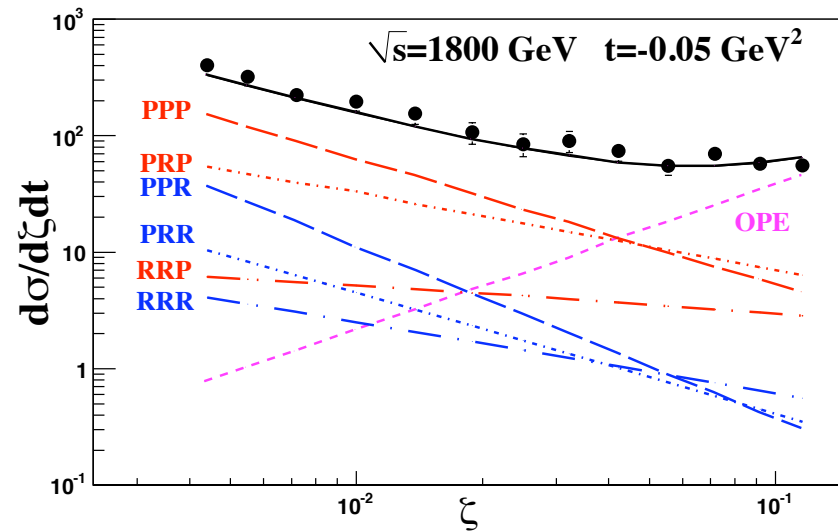
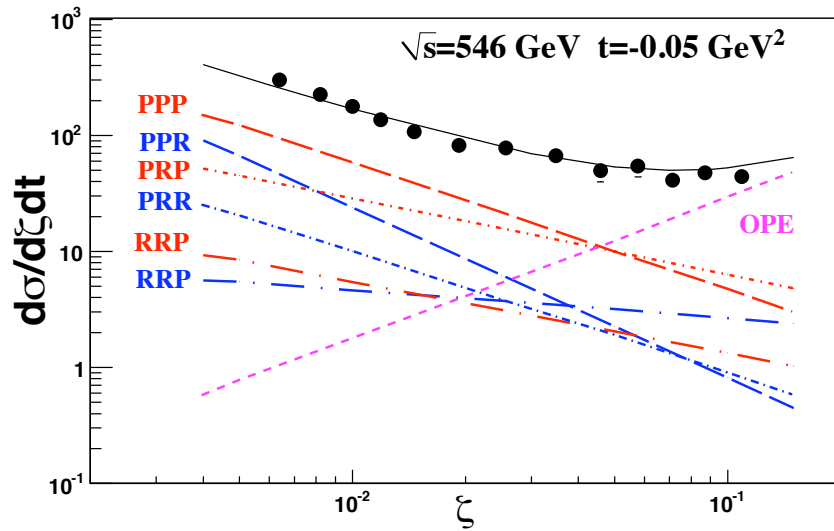
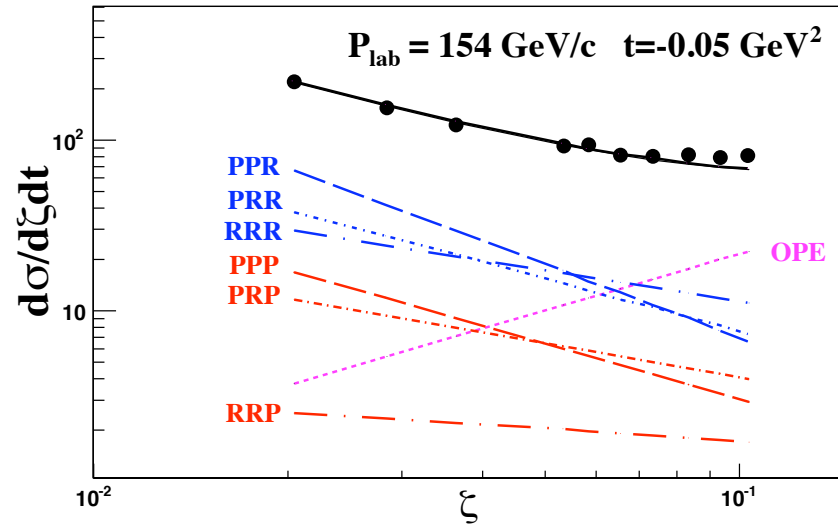
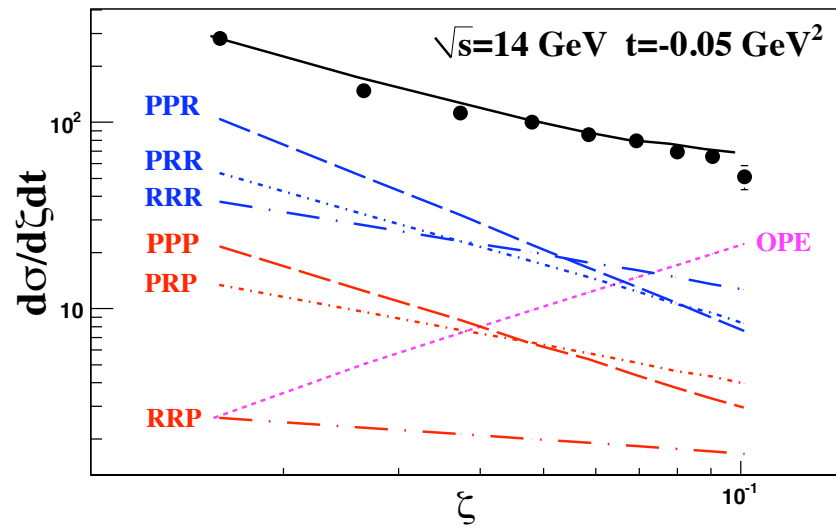


Cool et al. PRL 47

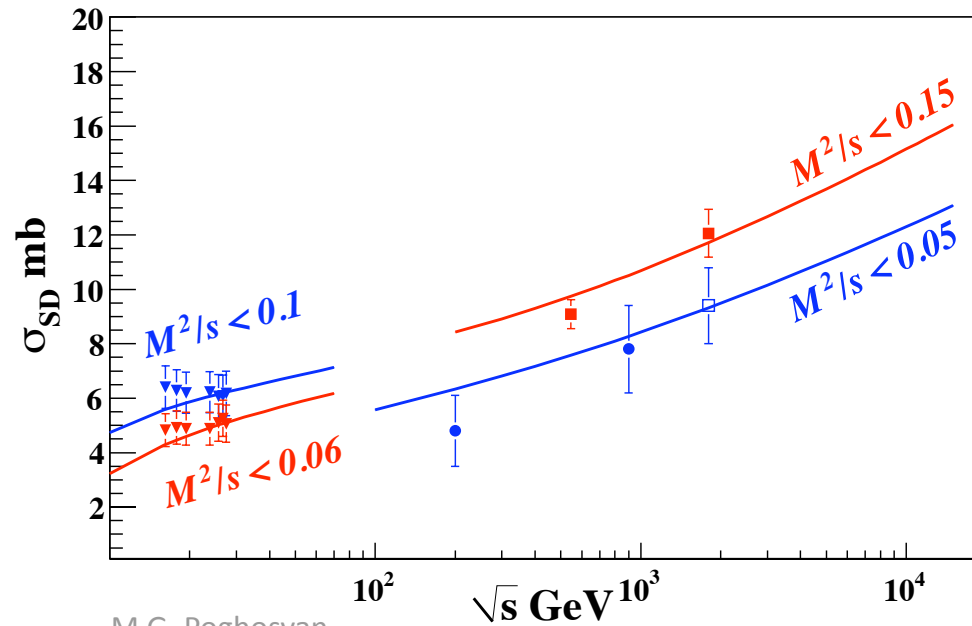
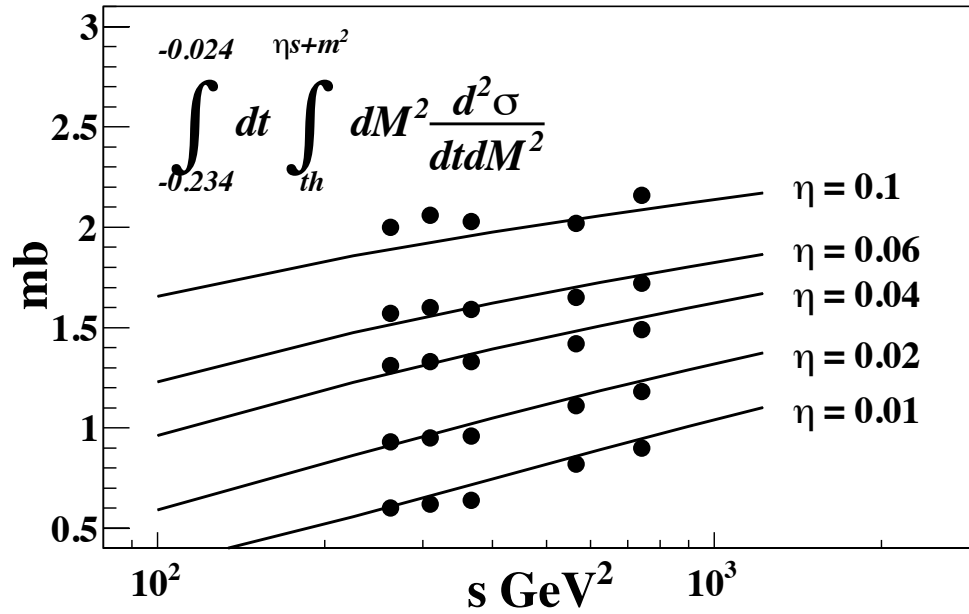


Goulianos, Montanha PR D59

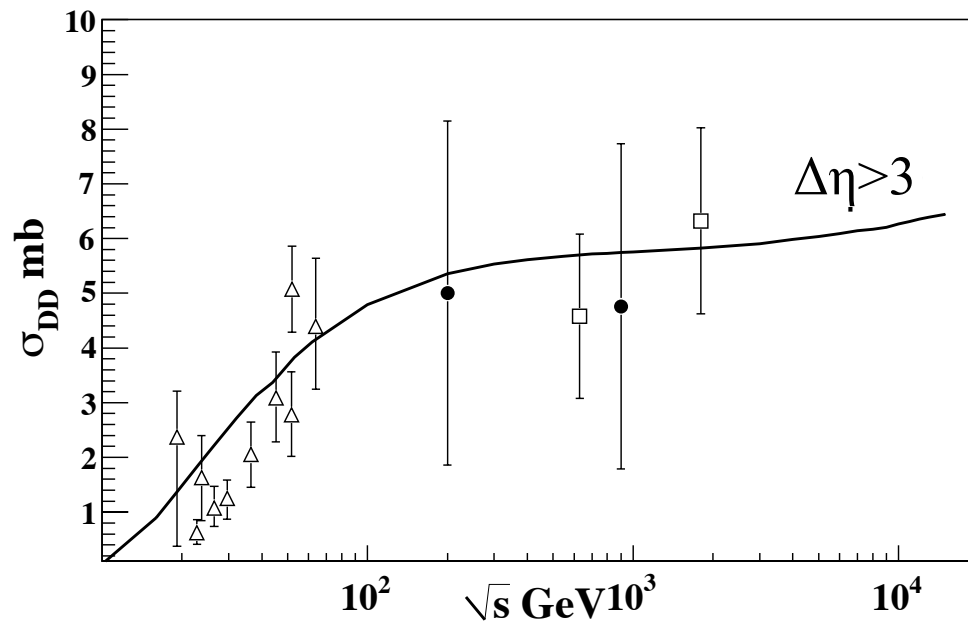
Evolution of the different therms.



Integrated SD cross-section



Integrated DD cross-section



Conclusion and predictions for LHC.

The model is simple but it gives a good description of data on soft diffraction dissociation.

\sqrt{s} TeV	σ_{tot} mb	σ_{el} mb	B GeV ⁻²	$\sigma_{SD}(M^2/s < 0.05)$ mb	$\sigma_{DD}(\Delta\eta > 3)$ mb
0.9	66.8	14.6	15.4	8.2	5.7
10	102	27	19.8	12	6.2
14	108	29.5	20.5	13	6.4

Based on the results of KT-MP Pomeron intercept renormalization scheme, we expect to have up to 5% uncertainty due to enhanced diagrams for total and elastic cross-sections and up to 10% for diffractive dissociation cross sections.

Appendix: One-pion exchange. The OPER-model

In the one-pion exchange approach the inclusive production of a hadron c in the fragmentation region of hadron a at interaction with hadron b is described by the diagram shown in Fig 10. According to the OPER-model, which was developed in ITEP [25], the invariant cross-section corresponding to this diagram has the form:

$$E_c \frac{d\sigma_{ab \rightarrow cX}}{d^3p_c} = \frac{1}{16\pi^3} \frac{J_{\pi b}}{J_{ab}} V(t) |F_\pi(s, s_x, t)|^2 \sigma_{\pi b}^{tot}(s_x) \quad (29)$$

In (29) $V(t) = \overline{|M_{a \rightarrow \pi c}|^2}$ represents the square of the $a\pi$ vertex function (averaged over initial spin states), where the pion is off-mass-shell. $J_{ab} = \sqrt{(p_a p_b)^2 - m_a^2 m_b^2}$, $J_{\pi b} = \sqrt{(q p_b)^2 - m_\pi^2 m_b^2}$. p_a, p_b, p_c and q are the 4-momenta of the a, b, c and the exchanged pion, respectively. $\sigma_{\pi b}^{tot}(s_x)$ is the on-mass-shell πb total cross-section.

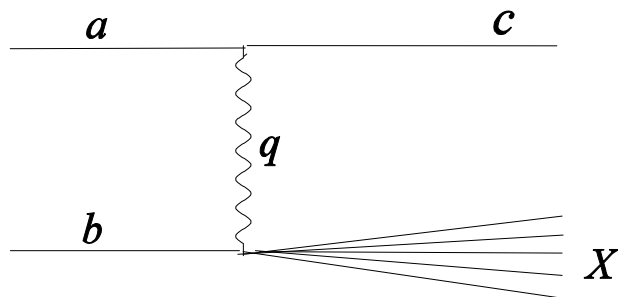
The formfactor $F_\pi(s, s_x, t)$ describing off-mass-shell corrections has the following form

$$F_\pi(s, s_x, t) = \exp\{\Lambda(t - \mu^2)\} \begin{cases} \frac{\pi}{2\sin(\alpha_\pi(t)\pi/2)}, & |t| < |t_0|, \\ \frac{\pi}{2\sin(\alpha_\pi(t_0)\pi/2)} \exp\{R_2^2(t - t_0)\}, & |t| \geq |t_0|. \end{cases} \quad (30)$$

$$\Lambda = R_1^2 + \alpha'_\pi \ln \frac{s}{s_x}; \quad \alpha_\pi(t) = \alpha'_\pi \cdot (t - \mu^2); \quad \alpha'_\pi = 1 \text{ GeV}^{-2}. \quad (31)$$

μ is the pion mass. In the region of the threshold masses of πN -scattering ($s_x \leq 2 \text{ GeV}^2$), where the P -wave production of $\Delta(1232)$ -resonance dominates, the amplitude is multiplied by the additional factor

$$f_\Delta(s_x, t) = \begin{cases} \frac{g_t}{g_0} \exp\{R_3^2(t - \mu^2)\}, & |t| < |t_0|, \\ \frac{g_0}{g_0} \exp\{R_3^2(t_0 - \mu^2) + R_4^2(t - t_0)\}, & |t| \geq |t_0|. \end{cases} \quad (32)$$



with

$$q_t = Q(s_x, m_N^2, t), \quad q_{t_0} = Q(s_x, m_N^2, t_0), \quad q_0 = Q(s_x, m_N^2, \mu^2), \quad (33)$$

$$Q(x, y, z) = \sqrt{(x - y - z)^2 - 4yz} / 2\sqrt{x}. \quad (34)$$

It should be noted that the nearness of the pion pole to the physical domain of scattering allows one to fix the absolute normalisation of the cross-section at small $|t|$. The behaviour at large values of $|t|$ is determined by the formfactor (30), (32) which takes into account other exchanges, absorption corrections, etc. In this connection we must speak about an "effective" π -meson exchange, meaning the hadron system, whose interaction at small $|t|$ is well approximated by the pion exchange.

The parameters t_0 and R_i^2 are determined from the comparison with experimental data [26] and have the following values

$$t_0 = -0.7 \text{ GeV}^2, \quad R_1^2 = 0.3 \text{ GeV}^{-2}, \quad R_2^2 = 0.74 \text{ GeV}^{-2}, \quad R_3^2 = 2.75 \text{ GeV}^{-2}, \quad R_4^2 = -1.3 \text{ GeV}^{-2}. \quad (35)$$